

Research on Low-Density Parity-Check Decoding Algorithm for Reliable Transmission in Satellite Communications

Yuanzhi He ^{1,*} and Yaoling Wang ^{1,2}¹ Institute of Systems Engineering, Academy of Military Sciences, Beijing 100141, China² School of Telecommunications Engineering, Xidian University, Xi'an 710071, China

* Correspondence: he_yuanzhi@126.com

Abstract: Satellite communications face difficulties such as intensified environmental attenuation, dynamic time-varying links, and diverse business scenarios, which usually require channel coding schemes with high coding gain and high throughput. Low-density parity-check (LDPC) codes are dominant in satellite communication coding schemes due to their excellent performance in approaching the Shannon limit and the characteristics of parallel computing. The traditional weighted-Algorithm B decoding algorithm ignores the channel received information and involves frequent multiplication operations and iteration, which introduces the channel received information for hard-decision and constellation mapping processing. Meanwhile, we design the correlated reliability between the extrinsic information and the mapping processing information to improve the correctness of decoding. The multiplication operation in the iterative process can be replaced by the simple sum of the Hamming distance coefficient, the correlated reliability between the extrinsic information and the mapping processing information, and the extrinsic information frequency, thereby reducing the complexity and storage load of the system. The simulation results show that the presented MRALDPC algorithm can obtain about 0.4 dB performance gain, and the average number of iterations is reduced by 68% under a low SNR. The algorithm can achieve better error-correcting performance and higher throughput, providing strong support for reliable transmission of satellite communications.

Keywords: satellite communications; channel coding; LDPC code; multi-dimensional information iterative decoding; reliable transmission



Citation: He, Y.; Wang, Y. Research on Low-Density Parity-Check Decoding Algorithm for Reliable Transmission in Satellite Communications. *Appl. Sci.* **2024**, *14*, 746. <https://doi.org/10.3390/app14020746>

Academic Editors: Chun-Yen Chang, Cheng-Fu Yang, Charles Tijus, Teen-Hang Meen and Po-Lei Lee

Received: 25 November 2023

Revised: 27 December 2023

Accepted: 7 January 2024

Published: 15 January 2024



Copyright: © 2024 by the authors. Licensee MDPI, Basel, Switzerland. This article is an open access article distributed under the terms and conditions of the Creative Commons Attribution (CC BY) license (<https://creativecommons.org/licenses/by/4.0/>).

1. Introduction

Satellite communication technology is a communication system that uses artificial satellites as the relay and inter-satellite and satellite-to-ground links as transmission networks to obtain, transmit, and process space information [1]. At the same time, satellite communications have excellent coverage and communication capacity. Whether it is land, sea, or air, it can realize communication connections and fill the areas that cannot be covered by ground infrastructure. It is often used for disaster-relief emergency communication and the real-time transmission of battlefield information [2]. Due to the long distance of satellite communications, the signal will be significantly attenuated during transmission, and the communication link will be affected by weather conditions such as clouds and rain [3], resulting in a high bit error rate (BER). Channel coding technology, as a key underlying technology in communication systems, can improve anti-interference and reliability [4]. The essence of channel coding technology is to introduce some controllable redundancy in the transmitted information, and the receiver uses this redundancy to detect and recover the transmission error so as to ensure efficient and reliable data transmission.

In recent years, achieving high-speed and reliable transmission with limited hardware resources on satellite has become a core challenge in the development of satellite communication. Different encoding and decoding techniques can significantly reduce the signal-to-noise ratio (SNR) requirement under the same BER [5] ($SNR = 10\lg(P_s/P_n)$,

where P_s and P_n represent the effective power of the signal and noise, respectively), thereby reducing the transmission power of satellite communication equipment and making it possible to miniaturize. For example, in satellite navigation, every 1 dB of SNR gain brought about by channel coding is converted into profits of billions of dollars [6].

Low-density parity-check (LDPC) codes have the performance of approaching the Shannon limit [7], high coding gain, and strong anti-interference ability [8]. They have been incorporated into the channel coding standard by the consultative committee for space data systems (CCSDS). Compared with traditional RS codes and convolutional codes, LDPC codes have the advantages of a simple coding structure, easy hardware implementation, and a low decoding threshold [9]. Compared with Turbo codes, LDPC codes have low coding complexity and are more suitable for parallel high-throughput encoder–decoder design [10]. LDPC codes have flexible bit-rate structures [11] and low error levels [12] and meet the application scenario of satellite link communication, so they have been widely used in the field of satellite communications [13]. For instance, reference [14] presented a novel early termination stopping criterion for LDPC decoders that is based on detecting the periodicity of syndrome weight oscillations. This design can reduce computational energy and can be implemented to meet the energy resources of satellite communications. Reference [15] presented filtered orthogonal frequency division multiplexed LDPC codes, which can achieve a coding gain of 1.2 dB with a BER of 10^{-3} under moderate rain weather conditions and can be well applied to Ka-band satellite communications.

In reference [16], a decoding algorithm based on majority logic for non-binary low-density parity-check (NB-LDPC) codes was presented, including Algorithm B (AlgB) and weighted-Algorithm B (wtd-AlgB). The AlgB decoding algorithm only considers the extrinsic information frequency, and its performance is not as good as the performance of the wtd-AlgB decoding algorithm. The wtd-AlgB decoding algorithm combines the Hamming distance coefficient and the extrinsic information to form a reliable measure for hard-decision symbols. However, the algorithm requires frequent multiplication operations for each decision.

In order to meet the highly reliable transmission requirements for satellite communications, this paper presents a new decoding algorithm based on multi-dimensional reliable information addition iteration (MRAI-LDPC). The main innovation of the MRAI-LDPC algorithm is as follows: Firstly, the Hamming distance coefficient is directly calculated by subtraction, avoiding its computer simulation process. Then, the channel received information is subjected to hard-decision and constellation mapping processing, and we design correlated reliability between the extrinsic information and the mapping processing information to improve the correctness of decoding. Finally, the Hamming distance coefficient, the correlated reliability between the extrinsic information and the mapping processing information, and the extrinsic information frequency are simply summed to reduce the system's complexity. The simulation results show that the presented MRAI-LDPC algorithm can achieve better error-correcting performance and throughput, ensuring the reliable transmission of satellite communications.

The remaining sections of this paper are organized as follows: Section 2 introduces the system model of LDPC. Section 3 designs a new LDPC decoding algorithm based on multi-dimensional reliable information addition iteration. In Section 4, we complete the performance simulation and complexity analysis of the MRAI-LDPC decoding algorithm. Finally, Section 5 provides a summary of this paper.

2. The System Model of LDPC

In satellite communications, signals may be affected by atmospheric fading, interference, and noise, resulting in transmission errors. LDPC codes have excellent error-correcting performance, which can effectively detect and correct errors during transmission, thus improving the reliability of communication systems. The constraint relationship between the check nodes and variable nodes of LDPC codes can be represented by the factor graph model in Figure 1. The factor graph model of LDPC mainly includes the variable

nodes (VNs), the check nodes (CNs), the parity-check matrix, and the side information connecting the variable nodes and the check nodes.

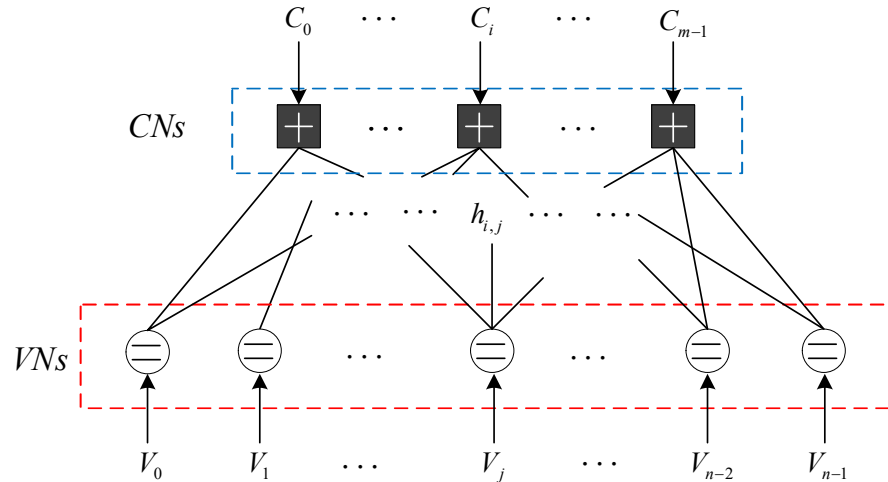


Figure 1. The factor graph model of LDPC.

Consider the regular NB-LDPC code $F_q[n, k]$ over $q = 2^r$. The code $F_q[n, k]$ is defined by a sparse parity-check matrix $\mathbf{H} = [h_{i,j}]_{m \times n} (h_{i,j} \in F_q)$, which has a constant row weight ρ and column weight γ . We design the set N_i of non-zero positions for the i -th row of \mathbf{H} by:

$$N_i = \{j : 0 \leq j \leq n - 1, h_{i,j} \neq 0\} \tag{1}$$

In Equation (1), for the i -th row, N_i is the set of $h_{i,j} \neq 0$ and j from 0 to $n - 1$ in \mathbf{H} . And we design the set M_j of non-zero positions for the j -th column of \mathbf{H} by:

$$M_j = \{i : 0 \leq i \leq m - 1, h_{i,j} \neq 0\} \tag{2}$$

In Equation (2), for the j -th column, M_j is the set of $h_{i,j} \neq 0$ and i from 0 to $m - 1$ in \mathbf{H} .

Assume that $\mathbf{c} = (c_0, c_1, \dots, c_j, \dots, c_{n-1}) \in F_q^n$ is a codeword to be transmitted. Each symbol c_j is converted to its binary representation by $\mathbf{c}_j = (c_{j,0}, c_{j,1}, \dots, c_{j,t}, \dots, c_{j,r-1}) \in F_2^r$, where $0 \leq j \leq n - 1$ and $0 \leq t \leq r - 1$. For simplicity, we only consider the additive white Gaussian noise (AWGN) channel with the binary phase-shift keying (BPSK) modulation. Each bit $c_{j,t}$ is modulated to a real sequence $\mathbf{x}_j = (x_{j,0}, x_{j,1}, \dots, x_{j,r-1})$ with constellation mapping rules $\phi(\bullet)$, where $x_{j,t} = \phi(c_{j,t}) = 1 - 2c_{j,t}$. The received signal $\mathbf{y}_j = (y_{j,0}, \dots, y_{j,t}, \dots, y_{j,r-1})$ is obtained from the modulated signal through the AWGN channel, where $y_{j,t} = x_{j,t} + n_{j,t}$ and $n_{j,t} \sim N(0, \sigma^2)$.

3. Design of LDPC Decoding Algorithm Based on Multi-Dimensional Reliable Information Addition Iteration

The wtd-AlgB decoding algorithm in reference [16] uses the advantage of the majority logic rule as a symbol decision, but it involves frequent finite-field multiplication and ignores the channel received information. To achieve a low-complexity and high-reliability decoding scheme, this paper presents a new LDPC decoding algorithm based on multi-dimensional reliable information addition iteration (MRAI-LDPC), which is described below.

3.1. Simplified Design of the Hamming Distance Coefficient

Let $\mathbf{z}^{(k)} = (z_0^{(k)}, z_1^{(k)}, \dots, z_{n-1}^{(k)})$ be the hard-decision information at the k -th iteration. At the same time, define the syndrome vector $\mathbf{s}^{(k)}$ at the k -th iteration by:

$$\mathbf{s}^{(k)} = \mathbf{z}^{(k)} \mathbf{H}^T = (s_0^{(k)}, s_1^{(k)}, \dots, s_{m-1}^{(k)}) \tag{3}$$

Here, $s_i^{(k)}$ represents the adjoint information of the i -th check node, which can be expressed as Equation (4). $z^{(k)}$ is a valid codeword if $s^{(k)} = \mathbf{0}$.

$$s_i^{(k)} = \sum_{j \in N_i} h_{i,j} z_j^{(k)} \tag{4}$$

Let $\sigma_{i,j}^{(k)}$ be the extrinsic information (EXI) from check node C_i to variable node V_j , which can be defined by:

$$\sigma_{i,j}^{(k)} = h_{i,j}^{-1} \sum_{j' \in N_i \setminus j} h_{i,j'} z_{j'}^{(k)} \tag{5}$$

In Equation (5), $0 \leq i \leq m - 1$ and $j \in N_i$. The check nodes only need to pass the EXI to its adjacent variable nodes in each iteration.

For the j -th variable node, $\bar{d}(z_j^{(k)}, \sigma_{i,j}^{(k)})$ is the Hamming distance between $z_j^{(k)}$ and $\sigma_{i,j}^{(k)}$. θ is $r + 1$ dimension vector with $\theta = (\theta_0, \theta_1, \dots, \theta_r)$, and $\theta_{\bar{d}(z_j^{(k)}, \sigma_{i,j}^{(k)})}$ is the Hamming distance coefficient, which is usually obtained by computer search with the goal of performance optimization [17]. However, it is difficult to find the optimal θ when the finite-field order is large.

Inspired by the method of calculating its initial reliability in reference [18], the Hamming distance coefficient $\theta_{\bar{d}(z_j^{(k)}, \sigma_{i,j}^{(k)})}$ can be simply designed as follows:

$$\theta_{\bar{d}(z_j^{(k)}, \sigma_{i,j}^{(k)})} = r - \bar{d}(z_j^{(k)}, \sigma_{i,j}^{(k)}) \tag{6}$$

In Equation (6), $r = \log_2 q$ and $\theta \in [0, r]$. Obviously, the smaller $\bar{d}(z_j^{(k)}, \sigma_{i,j}^{(k)})$ means that $\sigma_{i,j}^{(k)}$ is closer to $z_j^{(k)}$, indicating a higher reliability of $\sigma_{i,j}^{(k)}$, and the corresponding value $\theta_{\bar{d}(z_j^{(k)}, \sigma_{i,j}^{(k)})}$ should be obtained as a larger value. Moreover, the subtraction operation avoids the computer simulation and further reduces the complexity and storage load.

3.2. Design of the Correlated Reliability

In fact, the wtd-AlgB algorithm only considers the Hamming distance coefficient $\theta_{\bar{d}(z_j^{(k)}, \sigma_{i,j}^{(k)})}$ and the extrinsic information frequency $n(\sigma_{i,j}^{(k)})$ in each iteration and ignores the channel received information y_j . Generally speaking, y_j takes the value of a real number (including positive and negative decimals), while $\sigma_{i,j}^{(k)}$ is an integer within the range of a finite field. Obviously, the calculation between an integer and a real number will add an additional floating-point operation. In order to avoid floating-point operations in the algorithm, combined with the updated method $z_j^{(k)}$ of the iterative process in reference [19], the channel received information y_j is decided as follows:

$$z_{j,t}^{(0)} = \begin{cases} 0, & y_{j,t} \geq 0 \\ 1, & y_{j,t} < 0 \end{cases} \tag{7}$$

In Equation (7), if $y_{j,t} \geq 0$, the initial hard-decision vector $z_{j,t}^{(0)}$ is 0; otherwise, $z_{j,t}^{(0)} = 1$. In this step, the channel received information is introduced to improve the correctness of decoding, and the received real bit information is simplified to integer bit information, which is beneficial to reduce memory consumption.

Then, the constellation mapping rule $\phi(\bullet)$ is processed, and the mapping processing bit information is $w_{j,t} = \phi(z_{j,t}^{(0)}) = +1$ with $z_{j,t}^{(0)} = 0$; otherwise, $w_{j,t} = \phi(z_{j,t}^{(0)}) = -1$. In reference [20], the correlated reliability between the hard decision $z_j^{(k)}$ and the channel received information y_j is calculated. Similarly, in the j -th iteration, the correlated reliabil-

ity between the extrinsic information $\sigma_{i,j}^{(k)}$ and the mapped processing information w_j is computed by:

$$\rho(\sigma_{i,j}^{(k)}, w_j) = \sum_{t=0}^{r-1} \phi(\sigma_{i,j,t}^{(k)}) w_{j,t} \tag{8}$$

Here, $0 \leq j \leq n - 1$, and $\sigma_{i,j,t}^{(k)}$ is the binary expression of $\sigma_{i,j}^{(k)}$. Obviously, the larger the $\rho(\sigma_{i,j}^{(k)}, w_j)$, the more reliable the extrinsic information $\sigma_{i,j}^{(k)}$ is.

3.3. The Mechanism of Addition Operation

Since the wtd-AlgB algorithm has a large number of multiplication operations with $I(\sigma_{i,j}^{(k)}) = \theta_{\bar{d}(z_j^{(k)}, \sigma_{i,j}^{(k)})} n(\sigma_{i,j}^{(k)})$, it leads to an increase in resource consumption and energy consumption. To reduce the hardware resource on the satellite, the addition operation of $\theta_{\bar{d}(z_j^{(k)}, \sigma_{i,j}^{(k)})}$, $\rho(\sigma_{i,j}^{(k)}, w_j)$, and $n(\sigma_{i,j}^{(k)})$ can be expressed as:

$$M_j(\sigma_{i,j}^{(k)}) = [r - \bar{d}(z_j^{(k)}, \sigma_{i,j}^{(k)})] + \rho(\sigma_{i,j}^{(k)}, w_j) + n(\sigma_{i,j}^{(k)}) \tag{9}$$

In Equation (9), it is worth mentioning that each indicator is an integer and is positively correlated. The larger the total reliability $M_j(\sigma_{i,j}^{(k)})$, the more likely it is to be judged as $\sigma_{i,j}^{(k)}$.

For the j -th variable node, the updated variable node of the MRAI-LDPC decoding algorithm is shown in Figure 2. Bidirectional information transfer is carried out between the variable node V_j and the check node C_i . $z_j^{(k)}$ is passed to C_i through V_j , and C_i feeds back the total reliability $M_j(\sigma_{i,j}^{(k)})$ to V_j .

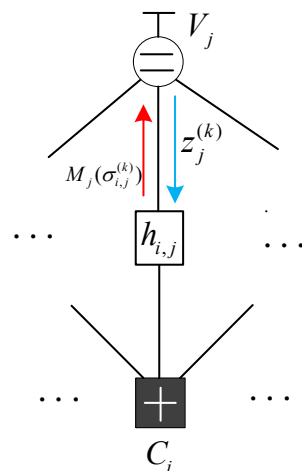


Figure 2. The updated graph of the j -th variable node.

Therefore, for the j -th variable node, the updated variable node of the MRAI-LDPC decoding algorithm is:

$$z_j^{(k+1)} = \begin{cases} \arg \max_{\sigma_{i,j}^{(k)}, i \in M_j} M_j(\sigma_{i,j}^{(k)}), & \max_{i \in M_j} M_j(\sigma_{i,j}^{(k)}) \geq T_H \\ z_j^{(k)}, & \max_{i \in M_j} M_j(\sigma_{i,j}^{(k)}) < T_H \end{cases} \tag{10}$$

In Equation (10), the optimal threshold value T_H is obtained by computer search.

As mentioned above, a new LDPC decoding algorithm based on multi-dimensional reliable information addition iteration (MRAI-LDPC) is designed as shown in Figure 3.

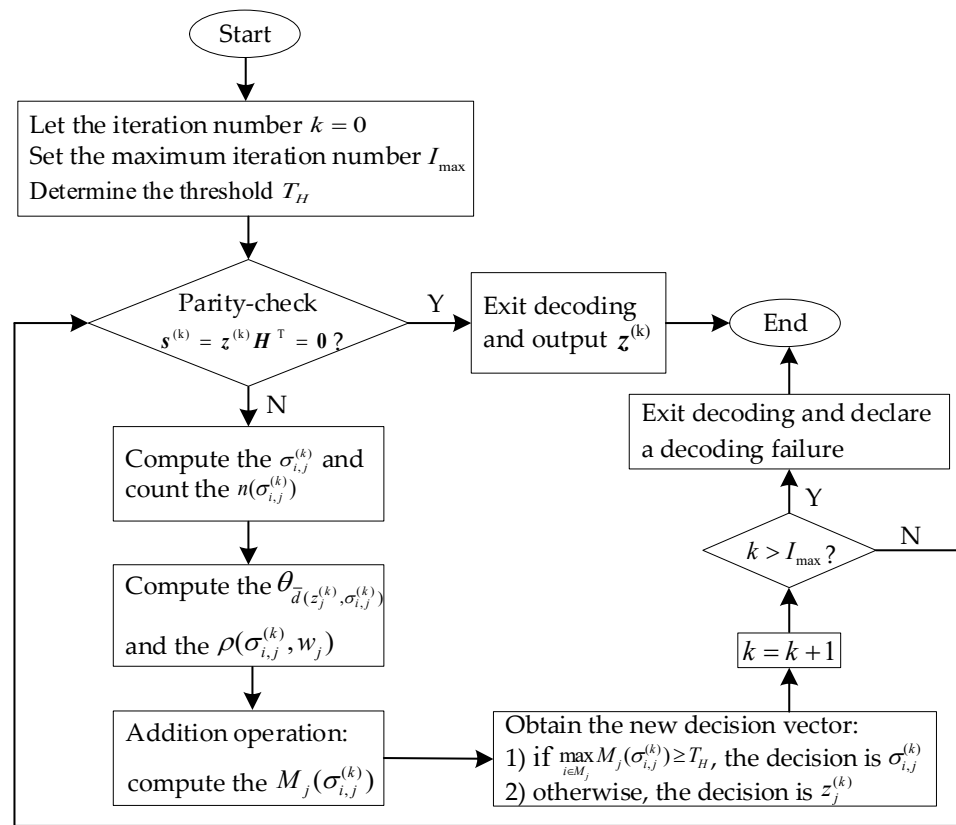


Figure 3. The flow diagram of the MRAI-LDPC decoding algorithm.

4. Simulation and Analysis of the MRAI-LDPC Decoding Algorithm

4.1. Decoding Performance

In this section, the performance of the presented MRAI-LDPC algorithm is simulated based on two quasi-cyclic LDPC codes (QC-LDPC) with different construction methods. The total frame number T_{total} is 10^8 , and the maximum iteration number I_{max} is 100. The algorithm stops decoding when T_{total} is more than 10^8 or I_{max} is more than 100.

4.1.1. Experiment 1

Consider the $F_{16}(225, 147)$ regular NB-LDPC code with finite-field construction [21], which has column weight $\rho = 14$, row weight $\gamma = 14$, and code rate $R = 0.65$. The parameters for several decoding algorithms are set as follows: (1) the threshold of the AlgB algorithm is set to 7; (2) for the wtd-AlgB algorithm, the threshold is set to 7 and the Hamming distance coefficient is $\theta = (2.1, 2.0, 1.0, 1.0)$; (3) for the presented MRAI-LDPC algorithm, the threshold T_H is set to 7. Meanwhile, we use the bit error rate (BER), the frame error rate (FER), and the average number of iterations (ANI) as the performance metrics. The BER and FER simulation results are shown in Figure 4.

The solid line in Figure 4 represents the BER performance, while the dashed line represents the FER performance. It can be seen from Figure 4 that:

- The BER performance and FER performance of the presented MRAI-LDPC algorithm are superior to the AlgB algorithm and the wtd-AlgB algorithm, thanks to the introduction of the channel received information, which improves the total reliability;
- The presented MRAI-LDPC algorithm achieves significant performance gains. For example, at a BER of 10^{-5} , the MRAI-LDPC decoding algorithm has about 0.4 dB BER performance gain over the wtd-AlgB algorithm. When FER is 10^{-4} , it has an FER performance gain of about 0.15 dB and 1.15 dB compared with the wtd-AlgB and wtd-AlgB algorithms, respectively;

- In addition, with the increase in SNR, the BER and FER of the MRAI-LDPC decoding algorithm decrease more rapidly, and the performance gain is more obvious.

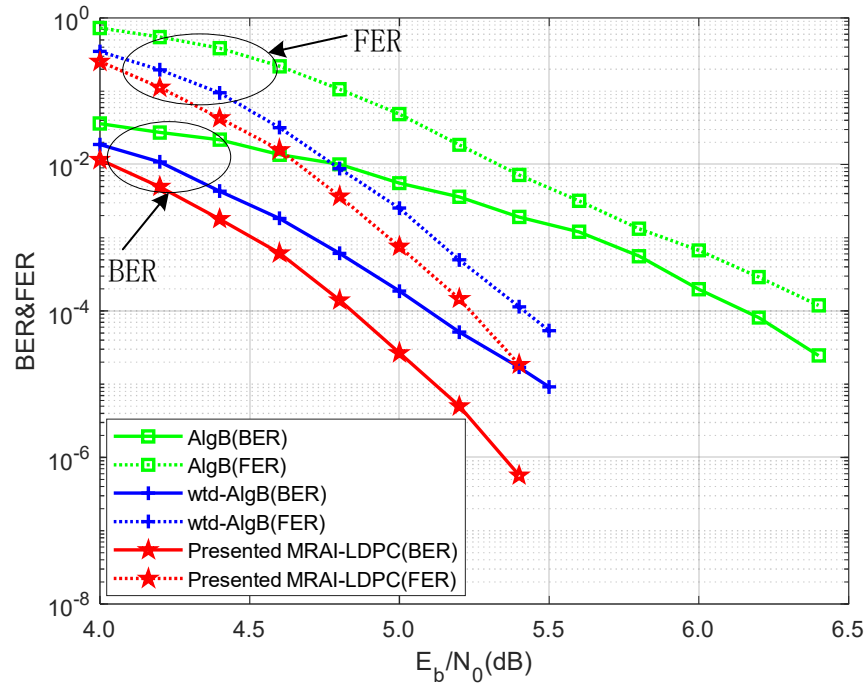


Figure 4. The BER and FER performance of the $F_{16}(225, 147)$ QC-LDPC code.

As depicted in Figure 5, the presented MRAI-LDPC algorithm has the fastest convergence speed among these decoding algorithms, especially in low SNR regions. For instance, at an SNR of 4.0~4.5 dB, the average number of iterations (ANI) of the MRAI-LDPC significantly decreases by 70~85% compared to the AlgB algorithm. When the SNR is 4.0 dB, the ANI of the wtd-AlgB algorithm is 38, while the MRAI-LDPC algorithm requires only 28 iterations on average.

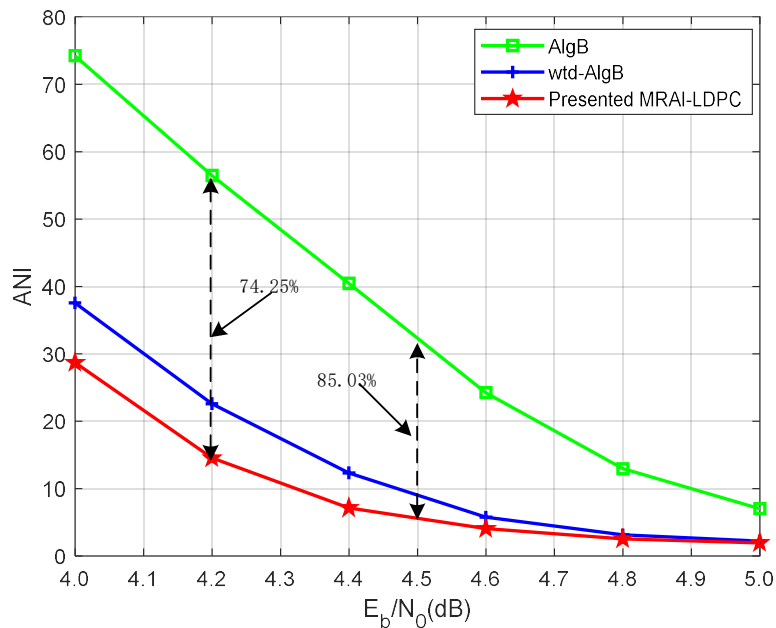


Figure 5. The average number of iterations under the $F_{16}(225, 147)$ QC-LDPC code.

4.1.2. Experiment 2

We also simulated the $F_{16}(255, 175)$ regular NB-LDPC code with a finite geometric construction [22]. This code has constant column weight $\rho = 16$, row weight $\gamma = 16$, and code rate $R = 0.68$. The parameters are set as follows: (1) for the AlgB algorithm, the threshold is set to 9; (2) the threshold and the Hamming distance coefficient are set to 9 and (2.1, 2.0, 1.0, 1.0) with the wtd-AlgB algorithm; (3) the threshold T_H of the presented MRAI-LDPC algorithm is set to 8.

Figure 6 depicts the decoding performance of the q-ary sum-product algorithm (QSPA) [23], AlgB decoding, wtd-AlgB algorithm, and MRAI-LDPC algorithm. Some results can be noted as follows:

- At a BER of 10^{-5} , the presented MRAI-LDPC algorithm has about 0.4 dB performance gain over the wtd-AlgB algorithm. Compared with the AlgB algorithm, the presented MRAI-LDPC algorithm can achieve a performance gain of about 1.35 dB with a BER of 10^{-4} ;
- When the SNR is greater than 4.5 dB, the BER curve of the MRAI-LDPC algorithm decreases faster, and the decreasing trend is almost the same as that of the QSPA algorithm.

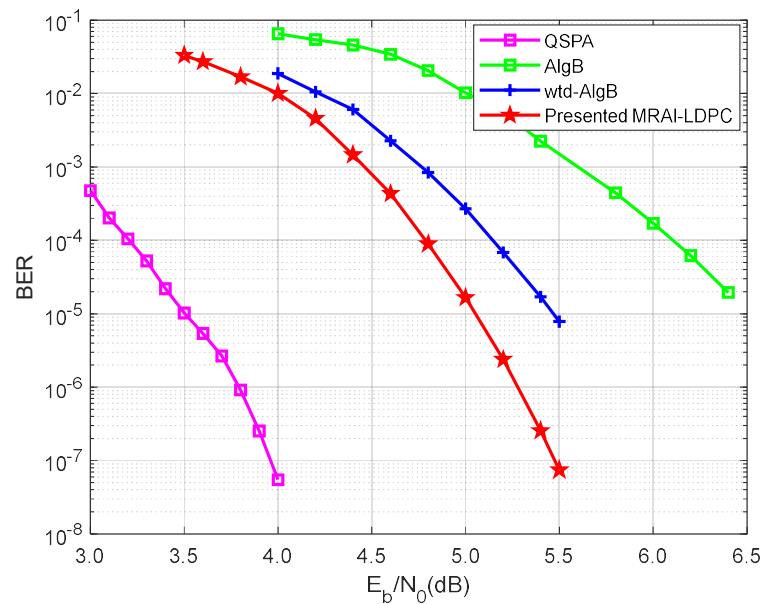


Figure 6. The decoding performance of the $F_{16}(255, 175)$ QC-LDPC code.

Additionally, we list the FER performance of the AlgB algorithm, the wtd-AlgB algorithm, and the MRAI-LDPC algorithm in Table 1. According to the numerical values, the FER of the MRAI-LDPC algorithm is smaller than that of the wtd-AlgB algorithm and the MRAI-LDPC algorithm under the same SNR, which indicates the presented MRAI-LDPC algorithm has the best error-correcting performance.

Table 1. The FER performance comparison of the $F_{16}(255, 175)$ QC-LDPC code.

SNR	AlgB Algorithm (FER)	wtd-AlgB Algorithm (FER)	MRAI-LDPC Algorithm (FER)
4.0 dB	0.6711409396	0.5602240896	0.2554278416
4.2 dB	0.5390835580	0.3241491086	0.1257071025
4.4 dB	0.3401360544	0.1877934272	0.0412116217
4.6 dB	0.2202643172	0.0714285714	0.0127575429

As can be clearly seen in Figure 7, the presented MRAI-LDPC decoding algorithm has the fastest ANI performance, and its average number of iterations is smaller than that of the AlgB and wtd-AlgB algorithms. At an SNR of 4.4 dB, the wtd-AlgB algorithm

requires about 22 iterations on average. In contrast, the MRAI-LDPC algorithm requires about 7, which means that the MRAI-LDPC reduces the average number of iterations by 68% compared with the wtd-AlgB algorithm.

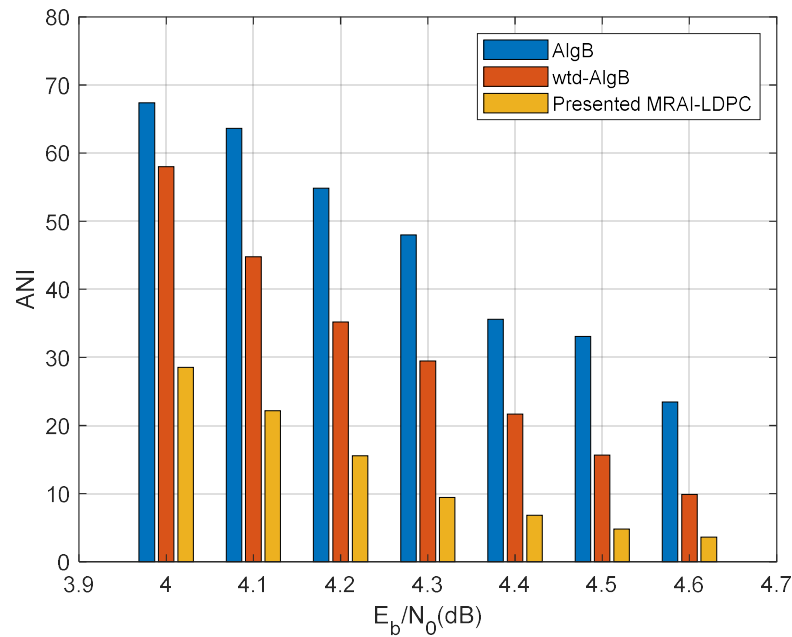


Figure 7. The ANI performance comparison of the $F_{16}(255, 175)$ QC-LDPC code.

4.2. Complexity Analysis

Here, we analyze the computational complexities of the presented MRAI-LDPC algorithm per iteration. The hard decision $z^{(k)}$ requires nr real comparisons (RCs). To compute the syndrome vector $s^{(k)}$, $n\gamma$ Galois-field multiplications (GMs) and $n(\gamma - 1)$ Galois-field additions (GAs) are required for computing. Then, $n\gamma$ GAs and $n\gamma$ GMs are required to obtain the extrinsic information $\sigma_{i,j}^{(k)}$. Counting the extrinsic information frequency $n(\sigma_{i,j}^{(k)})$ requires $n\gamma$ real additions (RAs). Additionally, the mapped processing information w_j is computed by nr RCs. It takes $n\gamma(r - 1)$ RAs to compute the correlated reliability $\rho(\sigma_{i,j}^{(k)}, w_j)$ between $\sigma_{i,j}^{(k)}$ and w_j . We require $3n\gamma$ GAs for computing the total reliability $M_j(\sigma_{i,j}^{(k)})$. Finally, updating the new decision vector involves $n(\gamma - 1)$ RCs in the MRAI-LDPC algorithm.

Let δ be the total edges of the nodes; note that $\delta = n\gamma = m\rho$. When an iteration is completed, 0 real multiplications (RMs), $5\delta - n$ GAs, 2δ GMs, δr RAs, and $\delta + n(2r - 1)$ RCs are required for the MRAI-LDPC algorithm. The total complexities are shown in Table 2. The MRAI-LDPC algorithm increases 2δ GA, $\delta(r - 1)$ RA, and $n(2r - 1)$ RC operations compared to the wtd-AlgB algorithm. However, lower energy consumption can be obtained in hardware implementation since the MRAI-LDPC algorithm does not involve the real-multiplication operation.

Table 2. Computational complexities per iteration with various decoding algorithms.

Decoding Algorithm	RM	GA	GM	RA	RC
wtd-AlgB	δ	$3\delta - n$	2δ	δ	δ
Presented MRAI-LDPC	0	$5\delta - n$	2δ	δr	$\delta + n(2r - 1)$

Under the simulation of the $F_{16}(225, 147)$ QC-LDPC code with finite-field construction, when the decoding is successful, the average number of iterations for the wtd-AlgB algorithm and the MRAI-LDPC algorithm is 9 and 5 at an SNR of 4.5 dB. The intuitive data

are given here, and the numerical results of the total computational complexities are shown in Table 3. Specifically, the total computational complexities of the MRAI-LDPC algorithm are 29,025 fewer than those of the wtd-AlgB algorithm.

Table 3. Total computational complexities of the $F_{16}(225, 147)$ QC-LDPC code.

Decoding Algorithm	RM	GA	GM	RA	RC	Total Operations
wtd-AlgB	28,350	83,025	56,700	28,350	28,350	224,775
Presented MRAI-LDPC	0	77,625	31,500	63,000	23,625	195,750

Column weight: $\rho = 14$; row weight: $\gamma = 14$ (SNR of 4.5 dB).

Similarly, under the $F_{16}(255, 175)$ regular NB-LDPC code and an SNR of 4.6 dB, the average number of iterations for the wtd-AlgB algorithm and the MRAI-LDPC algorithm is 10 and 4, respectively. According to the values in Table 4, compared with the wtd-AlgB algorithm, the total computational complexities of the MRAI-LDPC algorithm are reduced by 121,890, which greatly reduces the difficulty of hardware implementation.

Table 4. Total complexities under the $F_{16}(255, 175)$ QC-LDPC code.

Decoding Algorithm	RM	GA	GM	RA	RC	Total Operations
wtd-AlgB	40,800	119,850	81,600	40,800	40,800	323,850
Presented MRAI-LDPC	0	80,580	32,640	65,280	23,460	201,960

Column weight: $\rho = 16$; row weight: $\gamma = 16$ (SNR of 4.6 dB).

To summarize the results in Tables 3 and 4, it is clear that for a certain SNR, the presented MRAI-LDPC algorithm has the lowest complexity compared to the wtd-AlgB algorithm, which is an advantage that can reduce energy consumption and cost.

5. Conclusions

In view of the difficulties of satellite communication information transmission, such as increasing environmental attenuation and dynamic time-varying links, this paper presents a new LDPC decoding algorithm based on multi-dimensional reliable information addition iteration that realizes a satellite communication system with a fast transmission rate and efficient decoding while ensuring the reliability of satellite link communication. The existing wtd-AlgB decoding algorithm involves frequent finite-field multiplication, and its performance needs to be improved. In the MRAI-LDPC algorithm, we design a subtraction operation to calculate the Hamming distance coefficient. Then, the channel received information is introduced for hard-decision and constellation mapping processing. The correlated reliability between the extrinsic information and the mapped processing information is designed to promote the correctness of decoding. Finally, an addition operation is used to obtain total reliability, avoiding real-field multiplication operations and reducing hardware complexity and power consumption. The simulation results show that the MRAI-LDPC algorithm outperforms about 0.4 dB in performance and has fast convergence performance compared with the wtd-AlgB algorithm. Meanwhile, the average number of iterations is reduced by 68% to improve the system's throughput. The MRAI-LDPC algorithm has better error-correcting performance to ensure the reliability of information transmission. Moreover, we believe that it has application value in future satellite high-speed data transmission systems. It is worth mentioning that more research is needed on efficiently implementing this algorithm on field-programmable gate arrays (FPGAs).

Author Contributions: Conceptualization, Y.H. and Y.W.; methodology, Y.H. and Y.W.; software, Y.W.; validation, Y.H. and Y.W.; formal analysis, Y.H. and Y.W.; investigation, Y.W.; resources, Y.H.; data curation, Y.W.; writing—original draft preparation, Y.W.; writing—review and editing, Y.H.; visualization, Y.W.; supervision, Y.H.; project administration, Y.H.; funding acquisition, Y.H. All authors have read and agreed to the published version of the manuscript.

Funding: This research received no external funding.

Institutional Review Board Statement: Not applicable.

Informed Consent Statement: Not applicable.

Data Availability Statement: The data presented in this study are available on request from the corresponding author.

Conflicts of Interest: The authors declare no conflicts of interest.

References

1. Zheng, J.; Wang, R.; Li, Q.; Wang, X. Research on Key Technologies of Satellite Mobile Communication System. In Proceedings of the 2022 IEEE 5th International Conference on Electronics and Communication Engineering, Xi'an, China, 16–18 December 2022.
2. Liang, W.; Zeng, Y.; Zhu, W.; Shi, Z.; Li, X.; Liang, Y. Research on Beidou New Generation Emergency Group Communication Decision-Making Mechanism. In Proceedings of the 2022 IEEE 10th International Conference on Information, Communication and Networks, Zhangye, China, 23–24 August 2022.
3. Ahadi, S.; Baghersalimi, G. An OFDM-based GEO-satellite FSO Communications System Under Different Turbulent Regimes. In Proceedings of the 2022 13th International Symposium on Communication Systems, Networks and Digital Signal Processing, Porto, Portugal, 20–22 July 2022.
4. Venugopal, T.; Radhika, S. A Survey on Channel Coding in Wireless Networks. In Proceedings of the 2020 International Conference on Communication and Signal Processing, Chennai, India, 28–30 July 2020.
5. Fenech, H.; Amos, S.; Tomatis, A.; Soumpholphakdy, V. High throughput satellite systems: An analytical approach. *IEEE Trans. Aerosp. Electron. Syst.* **2015**, *51*, 192–202. [[CrossRef](#)]
6. Alvarez, A.; Fernandez, V.; Matuz, B. An Efficient NB-LDPC Decoder Architecture for Space Telecommand Links. *IEEE Trans. Circuits Syst. II* **2021**, *68*, 1213–1217. [[CrossRef](#)]
7. Mackay, D.J.C.; Neal, R.M. Near Shannon limit performance of low density parity check codes. *Electron Lett.* **1996**, *32*, 1645–1646. [[CrossRef](#)]
8. Chauvat, R.; Garcia-Pena, A.; Paonni, M. Efficient LDPC-Coded CCSK Links for Robust High Data Rates GNSS. *IEEE Trans. Aerosp. Electron. Syst.* **2023**, *59*, 404–417. [[CrossRef](#)]
9. Fang, Y.; Bi, G.; Guan, Y.L.; Lau, F.C.M. A Survey on Protograph LDPC Codes and Their Applications. *IEEE Commun. Surv. Tutor.* **2015**, *17*, 1989–2016. [[CrossRef](#)]
10. Song, L.; Yu, S.; Huang, Q. Low-density parity-check codes: Highway to channel capacity. *China Commun.* **2023**, *20*, 235–256. [[CrossRef](#)]
11. Zhang, C.; Mu, X.; Yuan, J.; Li, H.; Bai, B. Construction of Multi-Rate Quasi-Cyclic LDPC Codes for Satellite Communications. *IEEE Trans. Commun.* **2021**, *69*, 7154–7166. [[CrossRef](#)]
12. Li, G.; Fair, I.J.; Krzymien, W.A. Density evolution for nonbinary LDPC codes under Gaussian approximation. *IEEE Trans. Inform. Theory* **2009**, *55*, 997–1015. [[CrossRef](#)]
13. Koizumi, Y.; Suzuki, Y.; Kusunoki, T.; Yokohata, K.; Sujikai, H. Study on Error Correction in IP Network with LDPC Codes for Satellite Broadcasting and Coding Rate Conversion Method with Padding Bits. In Proceedings of the 2020 10th Advanced Satellite Multimedia Systems Conference and the 16th Signal Processing for Space Communications Workshop, Graz, Austria, 20–21 October 2020.
14. Vassallo, O.; Buttigieg, V.; Azzopardi, M.A. An Energy Efficient Hybrid FEC-ARQ Communication Scheme for Small Satellite Applications. In Proceedings of the 2021 International Conference on Computer, Information and Telecommunication Systems, Istanbul, Turkey, 11–13 November 2021.
15. Gumede, B.; Mukubwa, N.; Pillay, N.; Davidson, I.E. Performance Analysis of Filtered Orthogonal Frequency Division Multiplexed LDPC Codes for Satellite Communication in the Ka-Band. In Proceedings of the 2023 IEEE AFRICON, Nairobi, Kenya, 20–22 September 2023.
16. Jagiello, K.; Ryan, W.E. Iterative plurality-logic and generalized algorithm B decoding of q-ary LDPC codes. In Proceedings of the IEEE Information Theory and Applications Workshop, San Diego, CA, USA, 6–11 February 2011.
17. Huang, Q.; Zhang, M.; Wang, Z. Bit-reliability based low-complexity decoding algorithms for non-binary LDPC codes. *IEEE Trans. Commun.* **2014**, *62*, 4230–4240. [[CrossRef](#)]
18. Park, K.B.; Chung, K.-S. Iterative pseudo-soft-reliability-based majority-logic decoding for NAND flash memory. *IEEE Access* **2021**, *9*, 74531–74538. [[CrossRef](#)]
19. Li, X.; Qin, T.; Chen, H.; Sun, Y.; Liang, Q.; Luo, L. Hard-information bit-reliability based decoding algorithm for majority-logic decodable nonbinary LDPC codes. *IEEE Commun. Lett.* **2016**, *20*, 866–869. [[CrossRef](#)]
20. Wang, S.; Huang, Q.; Wang, Z.L. Symbol flipping decoding algorithms based on prediction for non-binary LDPC Codes. *IEEE Trans. Commun.* **2017**, *65*, 1913–1924. [[CrossRef](#)]
21. Zeng, L.Q.; Lan, L.; Tai, Y.Y.; Song, S.; Lin, S.; Abdel-Ghaffar, K. Constructions of nonbinary quasi-cyclic LDPC codes: A finite field approach. *IEEE Trans. Commun.* **2008**, *56*, 545–554. [[CrossRef](#)]

22. Zeng, L.Q. Constructions of nonbinary cyclic, quasi-cyclic and regular LDPC codes: A finite geometry approach. *IEEE Trans. Commun.* **2008**, *56*, 378–387. [[CrossRef](#)]
23. Davey, M.C.; MacKay, D.J.C. Low density parity check codes over $GF(q)$. *IEEE Commun. Lett.* **1998**, *2*, 165–167. [[CrossRef](#)]

Disclaimer/Publisher’s Note: The statements, opinions and data contained in all publications are solely those of the individual author(s) and contributor(s) and not of MDPI and/or the editor(s). MDPI and/or the editor(s) disclaim responsibility for any injury to people or property resulting from any ideas, methods, instructions or products referred to in the content.